

Chapter 4

Quantifying the Anthropogenic Signature in Drylands of Central Asia and Its Impact on Water Scarcity and Dust Emissions



Irina N. Sokolik, Alexander I. Shiklomanov, Xin Xi, Kirsten M. de Beurs, and Viatcheslav V. Tatarskii

4.1 Introduction: Anthropogenic Dust Assessments

Humans cause different impacts to the environment of Central Asia by modifying the water body and the land use which in turn resulted in emission of dust, known as the anthropogenic dust. The importance of anthropogenic impact to the global dust cycle has been increasingly recognized. However, it remains highly uncertain how much of the total dust emission or burden can be attributed to human activities in the atmospheric circulation and land surfaces (Tegen and Fung 1995; Sokolik and Toon 1996; Prospero et al. 2002; Mahowald and Luo 2003; Ginoux et al. 2012). Past estimates of the anthropogenic proportion of global dust vary from less than 10% to over 60% (Tegen and Fung 1995; Tegen et al. 2004; Mahowald and Luo 2003;

I. N. Sokolik (✉) · V. V. Tatarskii
School of Earth and Atmospheric Sciences, Georgia Institute of Technology,
Atlanta, GA, USA
e-mail: isokolik@eas.gatech.edu; vvt@eas.gatech.edu

A. I. Shiklomanov
Earth Systems Research Center, University of New Hampshire, Durham, NH, USA
e-mail: alex.shiklomanov@unh.edu

X. Xi
Department of Geological and Mining Engineering and Sciences,
Michigan Technological University, Houghton, MI, USA

K. M. de Beurs
Department of Geography and Environmental Sustainability, University of Oklahoma,
Norman, OK, USA
e-mail: kdebeurs@ou.edu

Ginoux et al. 2012; Stanelle et al. 2014). There are a number of reasons for such large uncertainties (Xi and Sokolik 2016). Firstly, there is no consensus on the definition of anthropogenic dust that has been used by the scientific community. There is a number of human activities that can directly or indirectly contribute to dust emission, such as agricultural practices over croplands and pasture, industrial and transportation activities, desiccation of rivers and lakes, and changes of precipitation and atmospheric circulation (Zender et al. 2004). Past studies considered various anthropogenic processes. Whether or not a dust source should be classified natural or anthropogenic depends on the time scope of the study. Secondly, there exist large differences in the model estimates of the magnitude of dust emissions, with even larger differences in the spatiotemporal distributions (Huneeus et al. 2011).

The representation of dust sources and model treatments of dust emission processes are the main sources of model errors (Knippertz and Todd 2012). In addition, the models represent only some mechanisms that control the complex dust emission. Various challenges are involved in separating natural and anthropogenic dust source areas. Satellite observations of land and vegetation properties have been widely used to characterize the extent and severity of land degradation (Le et al. 2016). Given that increased wind erosion is a direct sign of the desertification, land degradation maps provide useful information for locating potential human-made dust source areas (Zhang et al. 2003). The assignment of land degradation to human disturbance, meanwhile, is difficult because of various confounding factors from rainfall and soil moisture variations, vegetation phenology, and land management practices (Le et al. 2016). Instead, most relevant studies to date used global gridded agricultural fraction data to identify dust source areas that are caused by cultivation and livestock grazing (*e.g.* Tegen et al. 2004; Ginoux et al. 2012). Fourth, it remains controversial on how to treat anthropogenic dust sources in models. Tegen et al. (2004) suggested to reduce the erosion threshold velocity for cultivated soils, assuming that human disturbances make the soil more susceptible to erosion. In contrast, Ginoux et al. (2012) and Stanelle et al. (2014) increased the threshold velocity for croplands in order to account for the effects of soil conservation practices. These practices are generally part of model tuning to maximize the agreement between models and observations.

Significant cases of land degradations have occurred in Central Asia in the past century. Under the Soviet Union agricultural collectivization, Central Asia has experienced the expansion of cultivation and irrigation of the virgin lands from the early 1950s (Xi 2014; Kappas et al. 2020, Chap. 9). The Virgin Lands Campaign (1954–1960) has resulted into conversion of large areas of natural steppe into farmlands. These actions have caused severe wind erosion and catastrophic dust bowls due to the monoculture farming practice (Stringer 2008). The degraded lands were abandoned as a result, while more lands that are new were reclaimed. In addition, the nomadic pastoralism practices have been replaced by state and collective farms. The pasture lands have been grazed by an increasing large number of the livestock above the carrying capacity, year-round without migration. This has led to the depletion of the vegetation cover and upper soil layers, making the soil vulnerable to the

wind erosion (Gintzburger et al. 2005; Robinson et al. 2003). Following the collapse of Soviet Union, the production of cereal and grain underwent significant declines (Lioubimtseva and Henebry 2009; de Beurs and Henebry 2004). The livestock production system crashed and resulted in very steep declines in the livestock numbers and a slow recovery of the degraded pasture lands (Gintzburger et al. 2005; Wilson 1997).

The spatial distribution of cropland and pasture fractions and their annual changes from the 1950s and 2010s are shown in Fig. 4.1. We used the agricultural data from the Land Use Harmonization project (hereafter as LUH dataset, <http://luh.umd.edu/>). This dataset includes annual cropland and pasture fractions for the period of 1700–2005 at $0.5^\circ \times 0.5^\circ$ spatial resolutions (Hurt et al. 2011, 2006). A dry (or rainfed) crop belt of wheat and barley spreads eastward from Ukraine to the Ural Mountains and eastern Siberia, and southward to the Volga valley and northern Caucasus (Fig. 4.1) (Kappas et al. 2020, Chap. 9). The desert and steppe landscapes are being used as pasture lands, including the semi-arid steppe, shrublands and mountainous rangelands (Gintzburger et al. 2005). Irrigated croplands (*e.g.*, cotton, rice) are mainly located in loess deposits and river deltas of southern and southeastern mountains. Figure 4.1b shows the increasing cropland fraction from 10% in 1950 to 14% in 1960, likely due to cultivation of virgin lands. The fraction of cropland remains nearly constant until 1990. The cropland fraction has decreased after

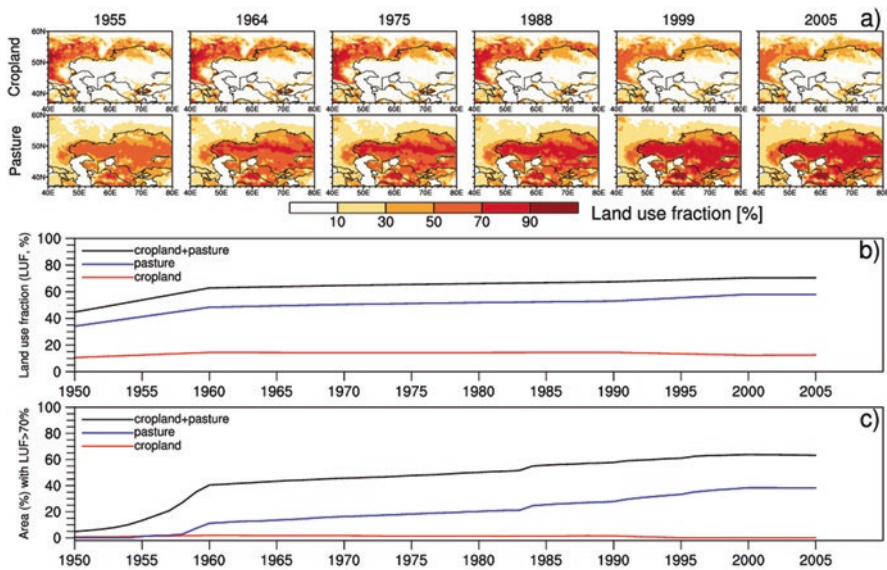


Fig. 4.1 (a) For selected years, shown are annual cropland and pasture fractions from the LUH dataset; (b) domain-average annual land-use fractions of cropland, pasture, and their sum (cropland+pasture), and (c) the percentage of land area with cropland plus pasture land-use fractions larger than 70%. (From Xi 2014)

1990, likely due to the Soviet Union collapse. In comparison, the pasture fraction has monotonically increased from 34% in 1950 to 48% in 1960 and to 58% in 2005. This indicates that the pasture fraction simply represents the fraction of the land area used for grazing, which does not reflect the decreasing trend of the grazing intensity following the Soviet Union collapse (Chen et al. 2020, Chap. 10). The cropland and pasture combined accounts for 45% of the total land surface in 1950 and 70% in 2005. Less than 2% of the total land area has a cropland fraction higher than 70%, whereas there are a lot more land areas that were mostly (fraction >70%) used as grazing lands.

Figure 4.2 shows the Landsat images for regional inland water bodies, illustrating significant water level variations in Central Asia (Le et al. 2016). As part of the agricultural collectivism policy, large-scale irrigation systems have been built to increase the soil fertility. As a result, the diversion of water from Amu Darya and Syr Darya caused the persistent shrinkage of the Aral Sea since the 1960s (Micklin 2007). By 2006, the Aral Sea has diminished by 90% in volume and 74% in area. The Aral Sea was separated into two parts in 1987: a small North Sea and a large south sea. The south Aral Sea includes a deep western basin and a shallow eastern basin with a narrow channel connecting them. The eastern basin suffered rapid desiccation in the last few years and became completely dry in 2014. The exposed sea bottom is a well-known dust source and is often referred to as Aralkum (Micklin

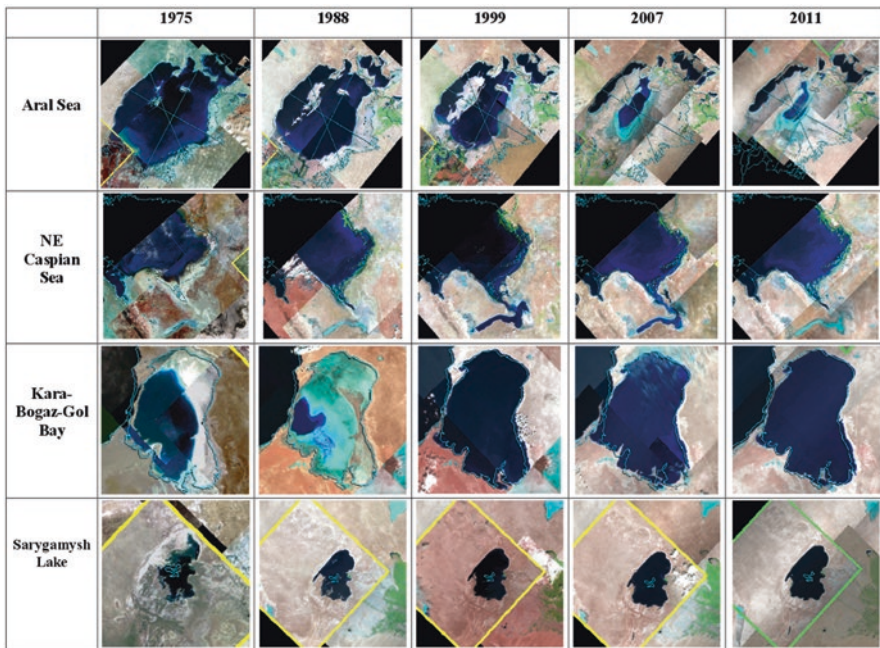


Fig. 4.2 Landsat images of surface water body changes. Shown are images for selected years (1975, 1988, 1999, 2007, and 2011). (From Xi 2014)

2007). The water level fluctuations of Caspian Sea has led to the drying (*e.g.*, 1975, 1988 and 2011) and inundation (*e.g.*, 1999, 2007) of the shallow northeast shoals (Kravtsova and Lukyanova 2000). As a result, the northeast Caspian coast turned into a dry solonchak desert which is undergoing wind erosion. A dam has been built in 1980 to block the water flow from Caspian Sea to the Kara-Bogaz-Gol bay, resulting in a dry salt flat prone to wind erosion (Leroy et al. 2006; Varushchenko et al. 2000). The Kara-Bogaz-Gol bay began to refill with water after the dam has been destroyed in 1992. In turn, the Sarygamysh Lake located to the southwest of Amu Darya has been progressively increasing in size due to the drainage water.

The land-use changes in Central Asia (*e.g.*, agriculture and water body) have significant consequence to the region’s dust emission, due to their impacts on the regional climate and land surface properties (Groisman et al. 2018). We developed a regional dust model system WRF-Chem-DuMo by employing the community Weather Research and Forecasting with chemistry (WRF-Chem) model. This modeling system enable us to examine the relationship between dust, climate, and land-cover/land-use change (Sokolik et al. 2013; Darmenova et al. 2009; Xi and Sokolik 2015). In WRF-Chem-DuMo model, the land surface is represented by a discrete number of dominant land cover (DLC) types. The DLC is defined as the land type in each grid cell with the largest fraction based on the 24-category US Geological Survey (USGS) Global Land Cover Characteristics Database (hereinafter USGS24). The USGS24 dataset is developed from the 1-year (April 1992–March 1993) Advanced Very High Resolution Radiometer NDVI data (Eidenshink and Faundeen 1994). Figure 4.3a shows that USGS24 mainly focuses on natural land types with no categories dedicated for agriculture, but instead use the mosaic classes of cropland and pasture. Because of its static nature, the data set has major representation errors of the present-day areal extent of Aral Sea and the shallow lagoon of Caspian

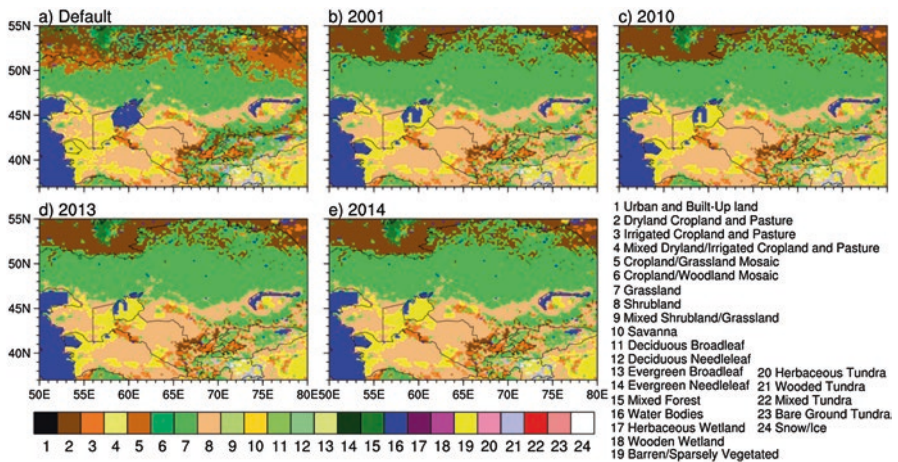


Fig. 4.3 (a) The default dominant land cover map in WRF-Chem-DuMo and (b–e) modifications for dust emission simulations (only 4 years are shown). (From Xi and Sokolik 2015)

Sea, the Kara-Bogaz-Gol (KBG) gulf (Xi and Sokolik 2016). The Aral Sea is incorrectly treated as a full lake, while the KBG gulf as a barren area. The KBG gulf was completely dry when a dam was built in 1980 to block water flow from the Caspian Sea. The dam was demolished in 1992, and after that the KBG gulf was refilled with water. As a result, the USGS24 data set needs to be modified to account for the changes in the land/water mask.

Here the LUH agricultural fraction data are used to reconstruct the spatial distribution of cropland and pasture in the USGS24 data set. The dust emission potential of the cropland and pasture lands depends on the threshold velocity as a function of the surface roughness properties and soil moisture. In the USGS24 DLC map, the cropland is presented as categories #2 “Dryland Cropland and Pasture” (hereafter referred to as CAT2) and #3 “Irrigated Cropland and Pasture” (CAT3), while pasture is represented by categories #7 “Grassland” (CAT7) and #8 “Shrubland” (CAT8). We modified the USGS24 cropland distribution based on the LUH cropland fraction. By considering all grid cells, the fraction of CAT2 or CAT3, depending on whether the grid is rainfed or irrigated cropland, is replaced by the LUH cropland fraction if the LUH cropland fraction is found to be larger than the CAT2 or CAT3 fraction (Xi and Sokolik 2015). Similarly, the fraction of CAT7 or CAT8 in each grid cell, depending on whether the grid is located north or south of 45°N, is replaced by the LUH pasture fraction, if the latter is found to be larger. Then, the fraction of the DLC type in each grid is subtracted to ensure that the fractions of all land types sum to 100%. Finally, a new DLC map is recomputed from the modified USGS24 land fractions. To correct the land/water mask, we modify the DLC type of the dried Aral Sea to “Barren/Sparsely Vegetated”, and the soil texture to “Silty Clay Loam”. We also modify the DLC type to “Water Bodies” in the KBG grid cells to reflect the restoration of KBG gulf. By modifying the cropland and pasture distributions and land/water mask, we are able to reconstruct the up-to-date USGS DLC maps. Figure 4.3 shows reconstructions for selected years (Table 4.1).

Our reconstructions include soil erosion at marginal lands under the Khrushchev’s virgin lands program, soil salinization due to excessive irrigation and poor drainage in cotton monoculture, desiccation of the Aral Sea, overgrazing of rangelands, abandonment of cultivated lands, and rehabilitation of overgrazed rangelands during the post-Soviet era (Gupta et al. 2009). Additionally, the region has experienced

Table 4.1 List of modelling experiments, indicating the abbreviated name of the experiment, dust seasons considered, the dust scheme used, soil size distribution used in the modeling, and wind used as a threshold value

Experiment	Dust seasons	Dust source function	Dust scheme	Soil size distribution	Wind
MB_Dry	2000–2014	–	MB	Dry-sieved	u_*
MB_Wet	2000–2014	–	MB	Soil texture	u_*
Shao_Dry	2000–2014	–	Shao	Dry-sieved	u_*
TF_Sta	2000–2014	Static	TF	–	u_{10}
TF_Dyn	2000–2008	Dynamic	TF	–	u_{10}

significant warming, but mixed changes occurred in precipitation with large impacts on the region’s glacier mass balance, streamflow, and agricultural production (Gupta et al. 2009; Lioubimtseva and Cole 2006). Although the enhanced wind erosion due to land-use activities in Central Asia is well documented (e.g. Orlovsky and Orlovsky 2002; Stringer 2008), there have been no quantitative assessments on its impacts on dust emission in the region.

Using the reconstructed land cover maps from multiple years (2000 to 2014), we conducted model simulations by employing the WRF-Chem-DuMo model to determine the contribution of direct land-use disturbance in agriculture and surface water bodies to the dust emission in Central Asia. We consider three dust emission schemes (including two physically based and one simplified), two soil size distributions, and two preferential dust source functions that for the five model experiments. Figure 4.4 shows the mapping of potential anthropogenic dust sources using four land use index (LUI) thresholds (80%, 85%, 90%, and 95%) at $1^\circ \times 1^\circ$ grid resolution, as

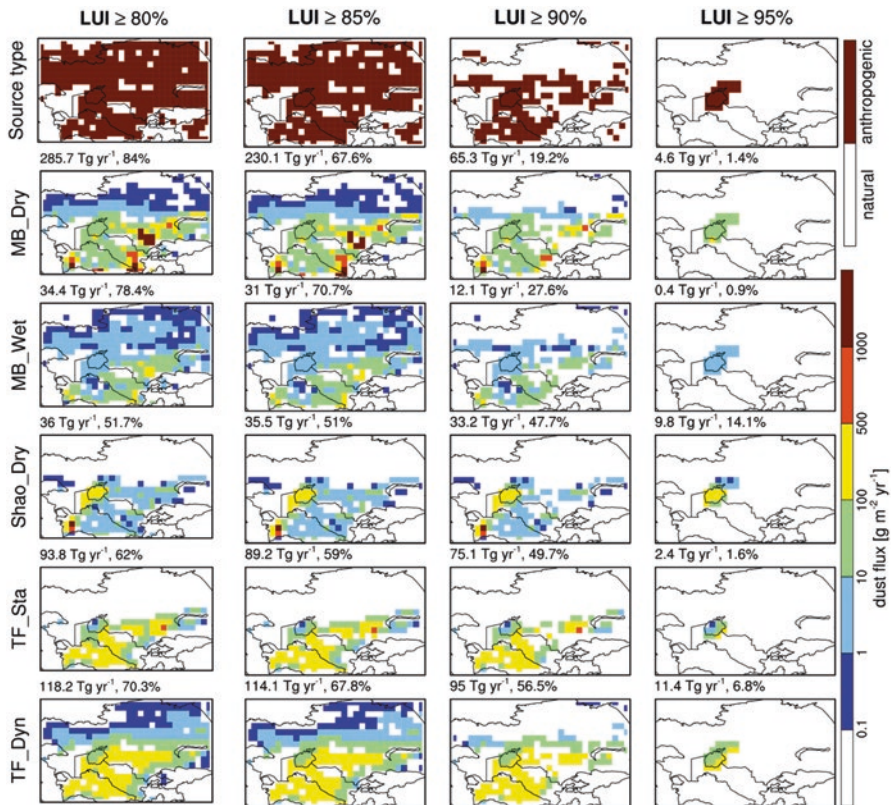


Fig. 4.4 Identification of anthropogenic dust source areas at $1^\circ \times 1^\circ$ grid resolution based on four LUI thresholds (80%, 85%, 90%, and 95%) and the corresponding anthropogenic dust fluxes based on MB_Dry, MB_Wet, Shao_Dry, TF_Sta, and TF_Dyn experiments. The domain-integrated annual anthropogenic dust fluxes (Tg year) and proportions (%) are also shown. (From Xi and Sokolik 2016)

well as the estimated anthropogenic dust fluxes based on the MB_Dry, MB_Wet, and Shao Dry experiments (Xi and Sokolik 2016). The majority of land surfaces are mapped as anthropogenic sources when using LUI thresholds of 80% and 85%. The source area is significantly reduced using a threshold of 90%, which covers an area of the semiarid steppe belt, Karakum and Kyzylkum deserts, and Aralkum. Aralkum becomes the only anthropogenic source when using a threshold of 95%. Based on long-term (1981–2006) satellite NDVI data, Le et al. (2016) found that Central Asian countries were subject to varying extent of land degradation (*e.g.*, 8% of the total land area in Turkmenistan and Uzbekistan, 60% in Kazakhstan). They identified several land degradation hotspots over croplands and grazing lands located in north Kazakhstan, northwest Tajikistan, and south Uzbekistan and Turkmenistan (see also Chen et al. 2020, Chap. 10). These hotspots are consistent with the anthropogenic source areas derived using the 90% LUI threshold, although the dust source areas are shifted toward grazing lands that have a higher LUI than croplands. Nevertheless, we consider the LUI threshold of 90% to offer a reasonable estimate of the anthropogenic dust source area in Central Asia. Based on five model experiments, 18.3–56.5% dust emission can be considered anthropogenic in Central Asia with an optimal LUI threshold of 90%. On the other hand, for the LUI threshold in the range of 85–90%, the ADP shows significant variations in the MB scheme (18.3–70.2%), but small changes in the Shao (32.8–48.1%) and TF (49.7–67.8%) schemes. Clearly, the different dust emission parameterizations not only cause a wide spread in the estimated anthropogenic dust proportions, but they are also responsible for the varying sensitivities of anthropogenic dust to the LUI threshold.

We detected a large model disparity from the five experiments considered in: (1) the estimated anthropogenic proportion of total dust emissions that ranged from 18.3% to 56.5%, (2) the spatial distribution of anthropogenic dust, (3) the sensitivity of anthropogenic dust to land-use intensity in separating natural and human-made source areas (Fig. 4.5), and (4) the relative importance of agriculture versus the

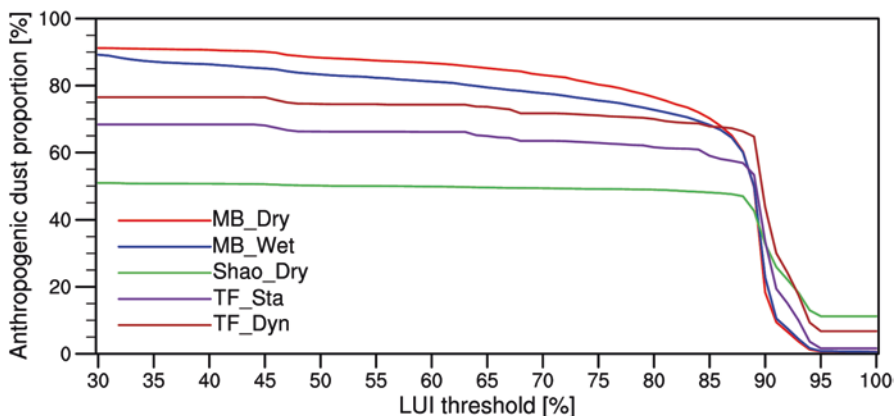


Fig. 4.5 The anthropogenic dust proportion as a function of the LUI threshold. (After Xi and Sokolik 2016)

desiccation of Aral Sea to the region's dust emission. We conclude that the parameterization of the model with erosion thresholds, particularly the vegetation effect on the threshold friction velocity, is a key source of model uncertainty in quantifying the contribution of human land use to dust emission. All model experiments show a negative trend in the anthropogenic dust proportion from 2000 to 2014, despite the continuous drying of Aral Sea that leads to enhanced dust activity in recent years. The decreasing trend points out to a shift of the dust emission toward natural source areas. Our model experiments also reveal consistent responses of anthropogenic dust to land-cover changes. We found that anthropogenic dust increases in response to the gain in the land type of open shrublands and decreases in response to the losses in grasslands and barren/sparsely vegetated. The overall resulting effect is a net decrease in the anthropogenic dust associated with land-cover changes over agricultural lands. In addition to the impacts of land-cover changes on dust emission, dust may also alter land cover by modifying the atmospheric radiation that affects the vegetation growth, and deposition processes, highlighting the need for an integrated understanding of human-dust-ecosystem interactions (*e.g.* Xi and Sokolik 2012; Farmer 1993).

4.2 Reconstruction of the Human Growth in the Region

World Bank (2017) reported a growth in more than 5000 cities in Eastern Europe and Central Asia in understanding city growth or decline (Restrepo Cadavid et al. 2017). The World Bank report included cities in Kazakhstan, Kyrgyzstan, Uzbekistan and Tajikistan, but most of the figures and graphs did not explicitly focus on these four countries. Here, we used the data from the World Bank report to explicitly investigate the urban growth in these four countries within our study area. We first investigated the urban growth between 1989 and 1999/2000; the population data is reported for slightly different years in these four countries. No population data for Tajikistan was available for the earliest time period (*i.e.*, no cities in this country in Fig. 4.6). We found that between 1989 and 1999/2000 most cities in Kazakhstan (51/73) declined in population, while the major hubs of Astana in the north and Almaty in the south experienced urban growth. Kyrgyzstan experienced a population decline in two thirds of its cities (18/27 cities). The situation appears very different in Uzbekistan, where a decline in the cities was only 10% (12/118).

During 1999/2000–2014, most cities in the study area grew (213/257), including Tajikistan (Fig. 4.7) and 88% growth in Uzbekistan. Kyrgyzstan and Kazakhstan cities also grew by 57% and 78%, respectively. While there is no data available for the first period in Tajikistan, there is data for this second period, which shows that 95% of the cities in Tajikistan grew between 2000 and 2014.

While increasing urban population is an indicator of growth, nightlight images can also illuminate human impact in a country. We downloaded the annual data for the years 1991, 2000 and 2013 from the version 4 DMSP OLS Nighttime Lights Time Series (NOAA Geophysical Data Center, 2018). This product presents persis-

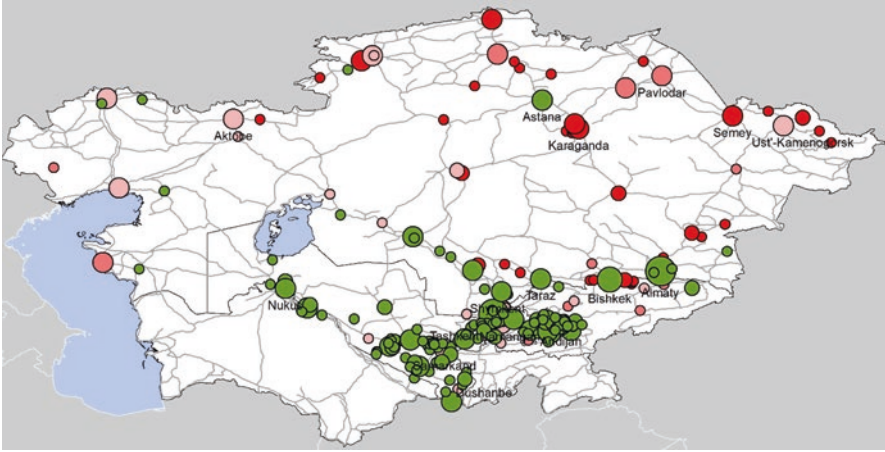


Fig. 4.6 City size based on the data from 1999/2000, change from 1989 to 1999

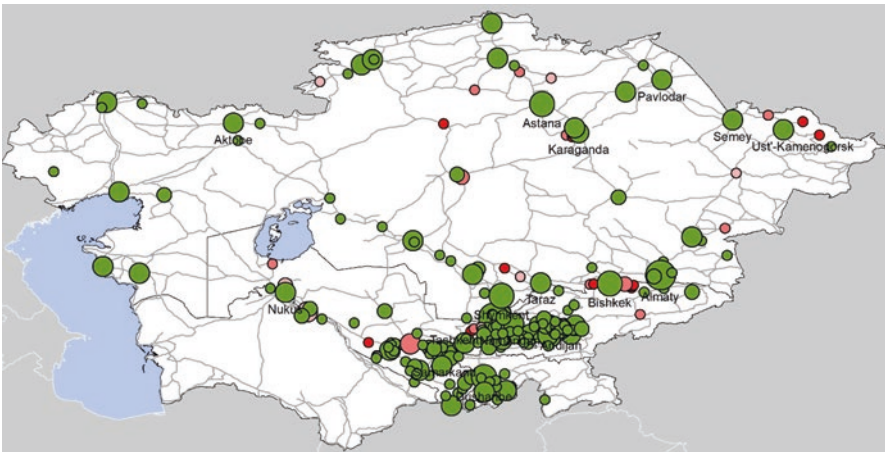


Fig. 4.7 City size based on data from 2014, change from 1999/2000 to 2014

tent lighting from cities, towns and other sites with background noise removed. The nightlight data shows that only a small portion of the land is lit at night in Central Asia, but rising from 4.5% in 1991 to 6.6% in 2013. It is interesting to note that the lit area grew in all countries between 1991 and 2000 in Central Asian countries, but between 2000 and 2013 both Tajikistan and Uzbekistan experienced a decline in the lit area (Table 4.2). At this point it is not clear why nightlights in these two countries declined.

We also investigated the rate of change in the intensity of the stable average lights product between 1991 and 2000 (Fig. 4.8-top) and from 2000 to 2013 (Fig. 4.8-bottom). We find that while the total percentage of lit land increased from

Table 4.2 Percentage of lit land area in Central Asian countries

	1991 (%)	2000 (%)	2013 (%)
Kazakhstan	3.1	3.4	5.0
Kyrgyzstan	3.4	6.0	9.0
Tajikistan	7.9	10.0	8.4
Turkmenistan	3.9	6.8	7.3
Uzbekistan	14.4	17.1	14.5
Central Asia	4.5	5.5	6.6

3.1% to 3.4% between 1991 and 2000 (Table 4.2), almost all lit areas in Kazakhstan declined in nightlight intensity (Fig. 4.8-top). The only areas with increasing nightlights are some of the core urban areas, the Kenkiyak oil fields south of Aktobe and another oil field to the north of Kyzylorda. This decline in night light intensity appears to match well with the decline in urban population in Kazakhstan during this period. Figure 4.4 also shows that the light intensity declined in Kyrgyzstan and Uzbekistan in both periods even though the urban population increased in almost all cities during that time (Fig. 4.7). In Kazakhstan on the other hand, the nightlight intensity increased between 2000 and 2013.

In a previous analysis, we applied the Seasonal Kendall trend test to time series of MODIS vegetation index data between 2001 and 2013 (de Beurs et al. 2015). We found a significant negative trend for almost 42% of the vegetated land surface in Kazakhstan. The other four Central Asian countries revealed much lower percentages of negative vegetation trends, with Uzbekistan presenting the next highest percentage (26.7%) and Tajikistan the lowest percentage of negative vegetation trends (4.1%). We found the highest percentage of negative vegetation trends (38.7%) in grasslands while the lowest percentage (22.4%) in areas with higher human influences (*e.g.*, croplands). We also mapped the vegetation index data against the human influence dataset (Wildlife Conservation Society-WCS and University 2005) and found that a majority of the negative changes occurred for areas with low/intermediate human influence. There were few areas with vegetation increases, but the areas that did increase were almost entirely collocated with areas of higher human influence.

4.3 Quantifying the Water Resources Used for the Agriculture

Central Asia and the Aral Sea drainage basin, in particular, have undergone devastating environmental alterations over the last half century due to land-use/land-cover change that resulted in severe ecological challenges. Water-related change involves all of the key agents of change: land-use/cover change, pollution, over-exploitation of surface and groundwater, and climate change/variability. The entire

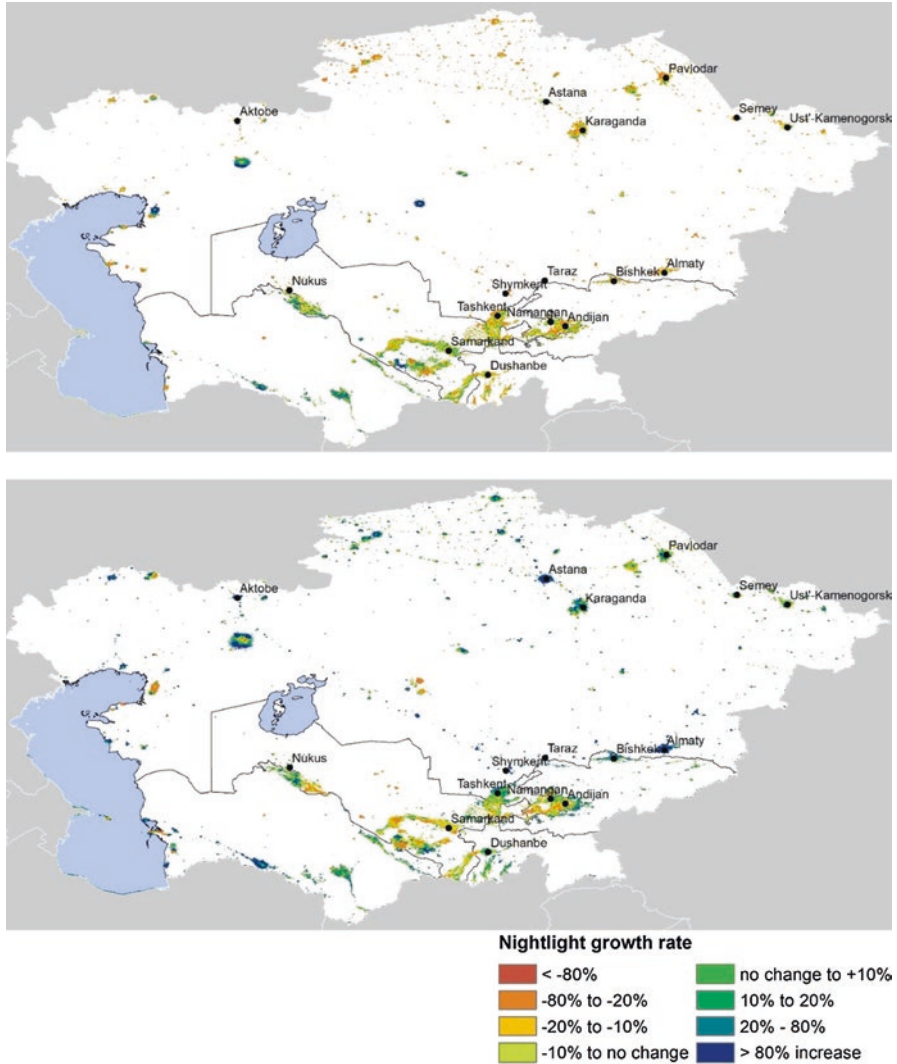


Fig. 4.8 (Top) Growth rate in nightlight intensity between 1991 and 2000; (Bottom) Growth rate in nightlight intensity between 2000 and 2013

Central Asian region is not water-scarce with total water resources and water availability per capita significantly greater than in the Northern Africa or the Near East. However, the territorial distribution of water resources in the region is spatially unequal. While the lowlands of the Aral Sea basin are characterized by deserts and semi-deserts, precipitation increases in the mountains, while the high mountains with their glaciers and permafrost areas serve as the “water towers” of the region. On average, 43% of the annual discharge in the basin originates in Tajikistan, 24%

in Kyrgyzstan, and approximately 19% in Afghanistan. However, the pattern of water usage is quite the opposite. The upstream mountain states use only about 17% of the water, while downstream Kazakhstan, Uzbekistan, and Turkmenistan use 83%.

The average total renewable water resources of the Central Asia is around 226 km³/year, including 46 km³/year inflow from neighboring countries, mainly China and Afghanistan (Shiklomanov and Rodda 2004). Most of regional renewable water resources are generated in the mountains where the largest regional rivers originate. Analysis of annual discharge variations for mountain rivers with relatively small human impact located in the Tianshan Mountains and the Syr Darya upstream basin showed significant upward trends for the most investigated rivers beginning in 90s (Chen et al. 2017). This tendency is observed downstream along the main channel of the Syr Darya River even though there is significant water use in the central part of the basin (Fig. 4.9). There are no, however, such obvious positive discharge trends for rivers located in the Pamir Mountains – Amu Darya upstream basin as well as for river gauges located along the main channel of the Amu Darya River (Fig. 4.9). The observed increasing tendencies in annual discharge of the Syr Darya river are mainly due to higher discharge rates in the spring and summer periods and are likely the result of more intensive snow and glacier melt driven by increasing regional air temperature in Tianshan mountains. Some decrease in area of irrigated lands especially in the Syr Darya river basin after the USSR breakup (Table 4.3) could also contribute to less agricultural water withdrawal and correspondingly higher streamflow (Qi et al. 2020, Chap. 5).

Climate change altering the regional hydrological cycle and fast population grows can significantly deteriorate the water availability in the region. Increase in

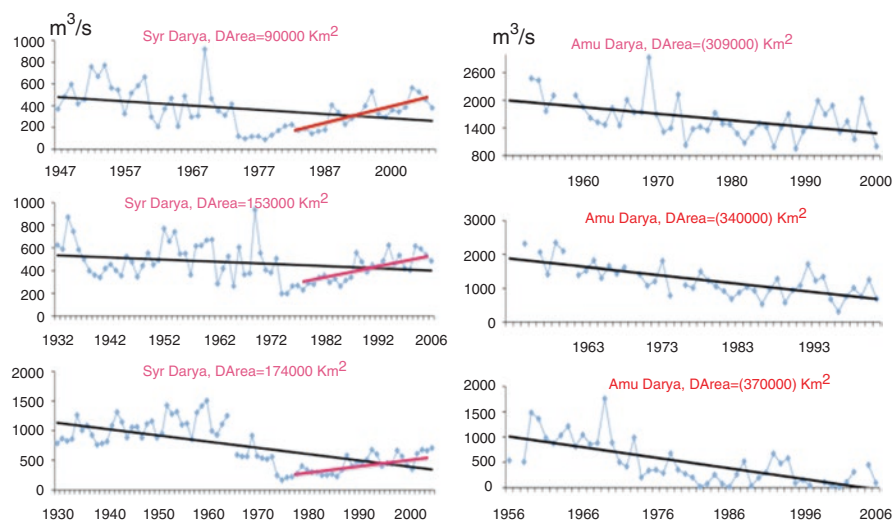


Fig. 4.9 Change in annual discharge along the main stem of Syr Darya (left panels) and Amu Darya rivers over the long-term period

Table 4.3 Area of irrigated lands by country (in thousand ha)

Country/year	1980	1990	1995	2000	2005	2010	2012
Kazakhstan	2690	2800	2681	2062	2127	2081	2100
Kyrgyzstan	1011	1004	1124	1064	1021	1021	1024
Tajikistan	671	751	747	750	800	762	748
Turkmenistan	850	1690	1780	1875	1990	1995	1995
Uzbekistan	3567	4187	4280	4256	4158	4350	4350
Total	8789	10,432	10,612	10,007	10,096	10,209	10,217

air temperature and associated accelerated glacier melt may eventually decrease river flows especially during vegetative period with serious consequences for regional agriculture, human security and development (Chen et al. 2020, Chap. 10). Recent estimate revealed the overall decrease from 1961 to 2012 in total glacier area and mass for the main regional mountain range – Tianshan to be $18 \pm 6\%$ and $27 \pm 15\%$, respectively (Farinotti et al. 2015). Meltwater from snow, glaciers and permafrost supplies around 80% of the total river runoff in Central Asia (Sehring and Diebold 2012). The mountain cryosphere is, therefore, a crucial source of water for irrigation agriculture as well as for hydropower production in the region (Groisman et al. 2020, Chap. 2).

4.3.1 Water Use for Agriculture

During USSR period the water use in the region was controlled by central government in Moscow. However, after independence, the contradictions between upstream and downstream countries of the Aral Sea drainage basin for water use were escalated. The resource endowments of upper and downstream countries in the Central Asia are much different; the two upstream countries of Kyrgyzstan and Tajikistan lack of oil and gas resources but with abundant water resources to produce a cheap hydropower energy, which is most required during winter period. The downstream countries – Uzbekistan, Kazakhstan and Turkmenistan – are short of runoff yields but producing large quantities of coal, petroleum, natural gas and other mineral resources, and have extensive production, which requires lots of water for irrigation during vegetative period. Thus, different interests of upstream and downstream countries in use of transboundary water resources may lead to regional conflicts (Chen et al. 2020, Chap. 10).

The Central Asian countries have one of the largest irrigation schemes in the world. Around 22 million people depend directly or indirectly on irrigated agriculture in the region. Twelve to forty percent of the GDP of the Kazakhstan, Kyrgyzstan, Uzbekistan, Turkmenistan and Tajikistan is derived from agriculture, which is mostly irrigated. Without irrigation, much of the agricultural land would revert to desert scrub. While some areas have been irrigated for centuries, many

irrigational schemes were developed in the 1950s–1980s to irrigate desert or steppe areas and hundreds of thousands of people moved to the areas to work in agriculture. During 1970–1989 irrigated area expanded by 150% and 130% in the Amu Darya and Syr Darya river basins respectively (World Bank 2003). The extensive agricultural water use has led to significant decline in river inflow to the Aral Sea and associated dramatic decrease in sea water level. The Aral Sea area shrunk from 65,000 km² in 1970s to 8000 km² in 2015 and has lost 90% of its volume during this period (Izhitskiy et al. 2016). A new salt saturated desert (AralKum) was formed on the former sea bed providing an additional important source for dust and salt storms in the region (Low et al. 2013). Irrigation continues playing an important role in the economies of Central Asian countries. Table 4.3 demonstrates the changes in area of irrigated lands by country area over 1980–2013 based on information published in local statistical reports and provided by our local collaborators. The total irrigated area in the region slightly decreased between 1995 and 2005 after the USSR breakup and it started increasing again since 2005. There are, however, very different patterns of the change within the region reflecting various socio-economic, demographic and political influences (Fig. 4.10). Water for agricultural needs was and continues to be used highly inefficiently in the region. For example, according to World Bank data, farmers in Uzbekistan withdraw an average of 14,000 m³/ha of water for irrigation, whereas rates in other countries with non-efficient irrigation such as Pakistan and Egypt are around 9000–10,000 m³/ha. Central Asian countries have one of the highest rates of water consumption per capita in the world from 1304 m³ in Kazakhstan to 5415 m³ in Turkmenistan, whereas the rates in USA and Israel are 1550 m³ and 281 m³, respectively. Extensive and non-efficient irrigation led to reduce the quality of farmland through lowering water tables and salinization.

4.3.2 Analysis of Changes in Regional Water Stress

The analysis of changes in water stress for Central Asia was performed using data collections and tools available at the Water Systems Analysis Group of the University of New Hampshire. The Water Balance Model – (WBM) was applied to understand the consequences of changes in climate, water use (Fig. 4.10a), demography, and economy on various variables and indices characterizing regional water security. The WBM accounts for sub-pixel land-cover types, glacier and snow-pack accumulation/melt across sub-pixel elevation bands, anthropogenic water use (*e.g.*, domestic and industrial water consumption, irrigation for most of existing crop types), and hydro-infrastructure for large inter-basin water transfer (*e.g.* Karakum Canal in the Central Asia) and reservoir/dam regulations (Grogan et al. 2015). The map shows Central Asian countries and sub-country administrative units (Fig. 4.10b). The census data about land use, crops and irrigated area from 1980 to 2014 for the administrative units were combined with gridded MIRCA2000 rainfed and irrigated crop

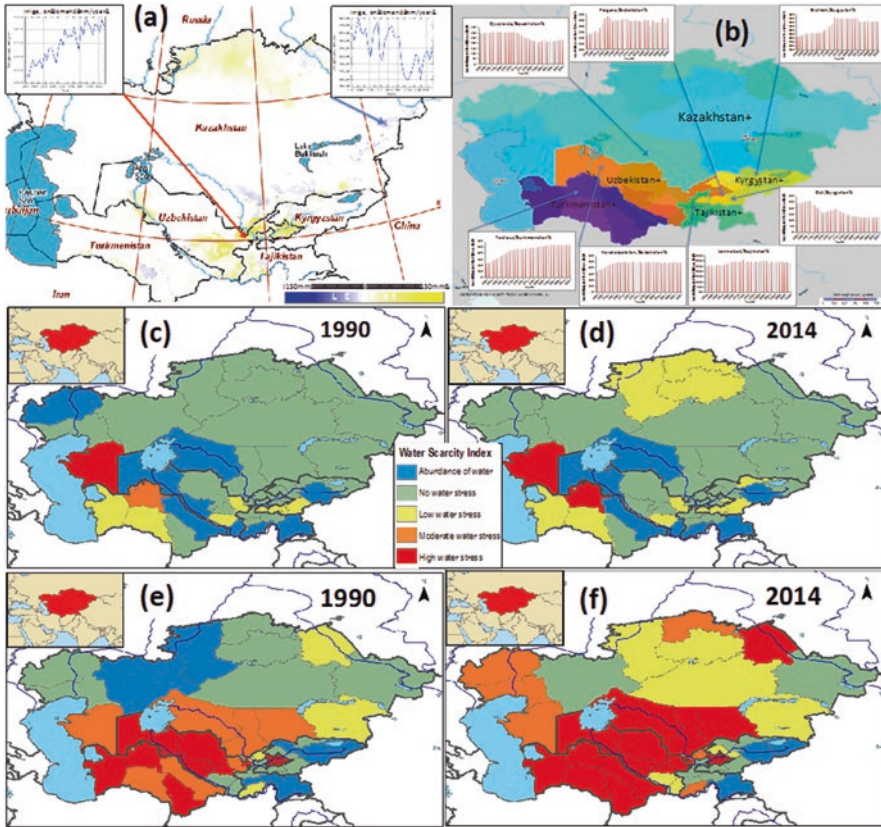


Fig. 4.10 Deviations in water use (irrigation, domestic, industrial, livestock) in mm/year between 2010–2014 and 1980–1985 are shown based on WBM simulations with 6 min spatial resolution; the embedded plots show opposite changes for two subregions (pixels) in annual water demand for irrigation (a); the map of administrative units of Central Asia and plots showing the dynamic of irrigated lands for several regions based on census data (b). Maps of Water Scarcity Index (WSI) based on total available water resources including inflow from other sub-regions (c, d), and only locally generated water resources (e, f) for 1990 and 2014. (From Shiklomanov et al. 2016)

data (Portmann et al. 2010) to provide variable land-use inputs for WBM simulations. The dynamics of water use for domestic, industrial and livestock needs were simulated in WBM using country-based statistical socio-economic information along with spatially distributed population density based on approach discussed in Shiklomanov and Rodda (2004).

The map (Fig. 4.10a) demonstrates the change in water use (via irrigation, domestic, industrial, livestock) across Central Asia between 2000–2012 and 1980–1985 based on WBM simulations using climatic data from MERRA- Modern Era Retrospective-Analysis for Research and Applications (Rienecker et al. 2011).

In general, the water use in the Central Asia has increased in 2000s from 1980 (yellow areas). Although in some regions of Kazakhstan, Kirgizstan and Turkmenistan the water use has declined, primarily due to decreased irrigation water demand. Two inserted plots show annual changes in irrigation water demand over 1980–2012 for two sub-regions (pixels) with opposite tendencies. Since 1980, irrigation water use significantly increased in Uzbekistan where the highest population growth rate has been observed. The barographs in Fig. 4.10b present official data about the changes in areas of irrigated lands for some administrative units. There are different patterns of the changes over 1980–2012, which reflect various socio-economic, demographic, and political issues. For example, significant drops in irrigated areas around 1990 in Osh region – Kyrgyzstan and Ferghana valley – Uzbekistan reflect the so-called Osh riots (ethnic conflict with numerous victims). Water Scarcity Index (WSI) (Brown and Matlock 2011) was estimated based on the WBM simulations using only locally generated water resources (Fig. 4.10e, f) and total available water resources (including inflow from other regions) (Fig. 4.10c, d). The index combines information about water abstractions and water availability. It is defined by the intensity of water resource use, *i.e.* the gross freshwater abstractions as percentage of the total renewable water resources or as percentage of internal water resources. This indicator is defined by the ratio $WSI=W/Q$, where W is the annual freshwater abstractions and Q is the annual available water. The severity of water stress is classified into several categories (from high water stress – red to abundance of water – blue Fig. 4.10c–f). This indicator neglects temporal and spatial variations as well as water quality. We also analyzed a number of other indexes and variables characterizing the water availability and water use in the region, including water availability index which compares all available water resources to the water demands (*i.e.* domestic, industrial and agricultural). There is general tendency towards significant decline in water availability by 2014 compared to 1990 (Fig. 4.10c–f). The water security situation in 2014 across the region is more stressful despite the significant political and socio-economic transformations in the region in 1990s, which led to a decrease in water use. This is primarily related to change in climatic conditions and population growth.

4.4 Conclusions

This chapter presents an analysis of the anthropogenic signature across the Central Asia. We examined the human influence on the LCLU dynamics and its consequences in the anthropogenic dust emission, water use, and the changes in urban growth. We used a regional dust modeling system WRF-Chem-DuMo to quantify the contribution of agricultural land use (*e.g.*, croplands and grazing lands) and desiccation of the Aral Sea to the dust emission in Central Asia between 2000 and 2014. We have also assessed the anthropogenic fraction of dust, defined as a fraction of dust that relates to various human activities.

Our findings suggest that the major source of uncertainties stems from the model parameterization of erosion thresholds, especially the vegetation effect on the threshold friction velocity. The model experiments reveal consistent responses of anthropogenic dust to occurring land-cover changes. In particular, the fraction of anthropogenic dust decreases in response to the gain in the land type of open shrublands and increases due to the losses in grasslands and barren/sparsely vegetated. The resulting effect is a net decrease in the anthropogenic dust associated with land-cover changes over agricultural lands. In addition to the impacts of land-cover changes on dust emission, dust may also alter land cover by influencing dryland ecosystems via radiative impacts and dust deposition processes, stressing the need for an integrated understanding of human-dust-ecosystem interactions.

We also investigated the rate of change in the intensity of the stable average lights product between 1991 and 2000 and from 2000 to 2013. Our analysis revealed that while the total percentage of lit land increased (3.1–3.4%) between 1991 and 2000 (Table 4.2) almost all lit areas in Kazakhstan declined in night light intensity (Fig. 4.8-top). The only areas with increasing nightlights are some core urban areas, the Kenkiyak oil fields south of Aktobe and another oil field to the north of Kyzylorda. This decline in night light intensity appears to match the decline in urban population in Kazakhstan during this period.

Water use has been a central factor in controlling the food security and the livelihood. Water is a key agent in Central Asia ultimately determining human well-being, food security, and economic development. There are complex interplays among the natural and anthropogenic drivers effecting the regional hydrological processes and water availability. Analysis of the data combined from regional censuses and remote sensing shows a decline in areas of arable and irrigated lands and a significant decrease in availability of arable and irrigated lands per capita across all Central Asian countries since the middle of 1990s as the result of post-Soviet transformation processes. This change could lead to considerable deterioration in food security and human system sustainability. The change of political situation in the region has also resulted in the escalated problems of water demand between countries in international river basins. Anthropogenic and Natural Systems (WBM-TrANS) has been used to understand the consequences of changes in climate, water and land use on regional hydrological processes and water availability. The model accounts for sub-pixel land-cover types, glacier and snow-pack accumulation/melt across sub-pixel elevation bands, anthropogenic water use (*e.g.*, domestic and industrial consumption, and irrigation for most of existing crop types), hydro-infrastructure for inter-basin water transfer and reservoir/dam regulations. We found that regional water availability is mostly impacted by the changes in extent and efficiency of crop field irrigation, especially in highly arid areas of Central Asia, changes in winter snow storage, and shifts in seasonality and intensity of glacier melt waters driven by climatic changes.

Acknowledgements This work has been supported by NASA LCLUC program, grant #NNX14AD88G.

References

- Brown A, Matlock MD (2011) A review of water scarcity indices and methodologies. White paper 106:19
- Chen Y, Li W, Fang G, Li Z (2017) Hydrological modeling in glacierized catchments of central Asia—status and challenges. *Hydrol Earth Syst Sci* 21(2):669
- Chen J, Ouyang Z, John R et al (2020) Social-ecological systems across the Asian Drylands Belt (ADB). In: Gutman G et al (eds) *Landscape dynamics of drylands across greater Central Asia: people, societies and ecosystems*. Springer, Cham
- Darmenova K, Sokolik IN, Shao Y, Marticorena B, Bergametti G (2009) Development of a physically based dust emission module within the Weather Research and Forecasting (WRF) model: assessment of dust emission parameterizations and input parameters for source regions in Central and East Asia. *J Geophys Res* 114(D14):D14201
- de Beurs KM, Henebry GM (2004) Land surface phenology, climatic variation, and institutional change: analyzing agricultural land cover change in Kazakhstan. *Remote Sens Environ* 89(4):497–509
- de Beurs KM, Henebry GM, Owsley BC, Sokolik I (2015) Using multiple remote sensing perspectives to identify and attribute land surface dynamics in Central Asia 2001–2013. *Remote Sens Environ* 170:48–61
- Eidenshink JC, Faundeen JL (1994) The 1 km AVHRR global land data set: first stages in implementation. *Int J Remote Sens* 15(17):3443–3462
- Farinotti D, Longuevergne L, Moholdt G, Duethmann D, Mölg T, Bolch T, Vorogushyn S, Güntner A (2015) Substantial glacier mass loss in the Tien Shan over the past 50 years. *Nat Geosci* 8(9):716
- Farmer AM (1993) The effects of dust on vegetation – a review. *Environ Pollut* 79(1):63–75
- Ginoux P, Prospero JM, Gill TE, Hsu NC, Zhao M (2012) Global-scale attribution of anthropogenic and natural dust sources and their emission rates based on MODIS Deep Blue aerosol products. *Rev Geophys* 50(3):0388
- Gintzburger G, Le Houérou HN, Toderich K (2005) The steppes of Middle Asia: post-1991 agricultural and rangeland adjustment. *Arid Land Res Manag* 19(3):215–239
- Grogan DS, Zhang F, Prusevich A, Lammers RB, Wissler D, Glidden S, Li C, Frohling S (2015) Quantifying the link between crop production and mined groundwater irrigation in China. *Sci Total Environ* 511:161–175
- Groisman PY, Bulygina ON, Henebry GM et al (2020) Dry land belt of Northern Eurasia: contemporary environmental changes. In: Gutman G et al (eds) *Landscape dynamics of drylands across greater Central Asia: people, societies and ecosystems*. Springer, Cham
- Gupta P, Kienzler K, Martius C et al (2009) Research prospectus: a vision for sustainable land management research in Central Asia. ICARDA Central Asia and Caucasus Program. *Sustainable Agriculture in Central Asia and the Caucasus Series No.1*. CGIAR-PFU, Tashkent
- Huneus N, Schulz M, Balkanski Y et al (2011) Global dust model intercomparison in AeroCom phase I. *Atmos Chem Phys* 11(15):7781–7816
- Hurtt GC, Frohling S, Fearon MG et al (2006) The underpinnings of land-use history: three centuries of global gridded land-use transitions, wood-harvest activity, and resulting secondary lands. *Glob Chang Biol* 12(7):1208–1229
- Hurtt GC, Chini LP, Frohling S et al (2011) Harmonization of land-use scenarios for the period 1500–2100: 600 years of global gridded annual land-use transitions, wood harvest, and resulting secondary lands. *Clim Chang* 109(1–2):117
- Izhitskiy AS, Zavialov PO, Sapozhnikov PV et al (2016) Present state of the Aral Sea: diverging physical and biological characteristics of the residual basins. *Sci Rep-UK* 6
- Kappas M, Degener J, Klinge M et al (2020) A conceptual framework for ecosystem stewardship based on landscape dynamics: case studies from Kazakhstan and Mongolia. In: Gutman G et al (eds) *Landscape dynamics of drylands across greater Central Asia: people, societies and ecosystems*. Springer, Cham

- Knippertz P, Todd MC (2012) Mineral dust aerosols over the Sahara: meteorological controls on emission and transport and implications for modeling. *Rev Geophys* 50(1):RG1007
- Kravtsova V, Lukyanova S (2000) Studies of recent changes in the Caspian coastal zone of Russia based on aerial and space imagery. *J Coastal Res*:196–206
- Le QB, Biradar C, Thomas R et al (2016) Socio-ecological context typology to support targeting and upscaling of sustainable land management practices in diverse global dryland. Paper presented at the 8th International Conference on Environmental Modelling and Software, Toulouse, France, July 11, 2016
- Leroy S, Marret F, Giralte S, Bulatov S (2006) Natural and anthropogenic rapid changes in the Kara-Bogaz Gol over the last two centuries reconstructed from palynological analyses and a comparison to instrumental records. *Quatern Int* 150(1):52–70
- Lioubimtseva E, Cole R (2006) Uncertainties of climate change in arid environments of Central Asia. *Rev Fish Sci* 14(1–2):29–49
- Lioubimtseva E, Henebry GM (2009) Climate and environmental change in arid Central Asia: impacts, vulnerability, and adaptations. *J Arid Environ* 73(11):963–977
- Low F, Navratil P, Kotte K et al (2013) Remote-sensing-based analysis of landscape change in the desiccated seabed of the Aral Sea—a potential tool for assessing the hazard degree of dust and salt storms. *Environ Monit Assess* 185(10):8303–8319
- Mahowald N, Luo C (2003) A less dusty future? *Geophys Res Lett* 30(17):017880
- Micklin P (2007) The Aral Sea disaster. *Annu Rev Earth Plant Sci* 35(1):47–72
- Orlovsky N, Orlovsky L (2002) White sandstorms in Central Asia, Global alarm: dust and sandstorms from the world's drylands. In: Youlin Y, Squires V, Qi L (eds) . UNCCD United Nations, Bangkok, pp 169–196
- Portmann FT, Siebert S, Döll P (2010) MIRCA2000 – global monthly irrigated and rainfed crop areas around the year 2000: a new high-resolution data set for agricultural and hydrological modeling. *Global Biogeochem Cy* 24(1)
- Prospero JM, Ginoux P, Torres O et al (2002) Environmental characterization of global sources of atmospheric soil dust identified with the NIMBUS 7 Total Ozone Mapping Spectrometer (TOMS) absorbing aerosol product. *Rev Geophys* 40(1):1002
- Qi J, Pueppke S, Kulmatov R et al (2020) The complexity and challenges and challenges of Central Asia's water-energy-food systems. In: Gutman G et al (eds) *Landscape dynamics of drylands across greater Central Asia: people, societies and ecosystems*. Springer, Cham
- Restrepo Cadavid P, Cineas G, Quintero LE, Zhukova S (2017) Cities in Eastern Europe and Central Asia: a story of urban growth and decline
- Rienecker MM, Suarez MJ, Gelaro R et al (2011) MERRA: NASA's modern-era retrospective analysis for research and applications. *J Clim* 24(14):3624–3648
- Robinson S, Milner-Gulland EJ, Alimaev I (2003) Rangeland degradation in Kazakhstan during the Soviet era: re-examining the evidence. *J Arid Environ* 53(3):419–439
- Sehring J, Diebold A (2012) *Water unites: from the glaciers to the aral sea*. Trescher Verlag
- Shiklomanov IA, Rodda JC (2004) *World water resources at the beginning of the twenty-first century*. Cambridge University Press
- Shiklomanov A, Prusevich A, Gordov EP et al (2016) A Environmental science applications with Rapid Integrated Mapping and analysis System (RIMS). *IOP Conf Ser Earth Environ Sci* 1:012034
- Sokolik IN, Toon OB (1996) Direct radiative forcing by anthropogenic airborne mineral aerosols. *Nature* 381(6584):681–683
- Sokolik IN, Darmenova K, Huang J et al (2013) Examining changes in land cover and land use, regional climate and dust in dryland East Asia and their linkages within the Earth system. In: Chen J, Wan S, Henebry G et al (eds) *Dryland East Asia: land dynamics amid social and climate change*. HEP – De Gruyter, Berlin, pp 185–213
- Stanelle T, Bey I, Raddatz T et al (2014) Anthropogenically induced changes in twentieth century mineral dust burden and the associated impact on radiative forcing. *J Geophys Res Atmos* 119(23):13526–13546

- Stringer LC (2008) From global environmental discourse to local adaptations and responses: a desertification research agenda for Central Asia. In: *The socio-economic causes and consequences of desertification in Central Asia*. Springer, Dordrecht, pp 13–31
- Tegen I, Fung I (1995) Contribution to the atmospheric mineral aerosol load from land surface modification. *J Geophys Res-Atmos* 100(D9):18707–18726
- Tegen I, Werner M, Harrison SP, Kohfeld KE (2004) Relative importance of climate and land use in determining present and future global soil dust emission. *Geophys Res Lett* 31(5):n/a–n/a
- Varushchenko AN, Lukyanova SA, Solovieva GD et al (2000) Evolution of the Gulf of Kara-Bogaz-Gol in the past century. In: Lulla KP, Dessinov LV (eds) *Dynamic earth environments: remote sensing observations from Shuttle-Mir Missions*. Wiley, pp 201–210
- Wildlife Conservation Society-WCS, University CFIESINCC (2005) Last of the wild project, Version 2, 2005 (LWP-2): global human influence Index (HII) Dataset (Geographic). NASA Socioeconomic Data and Applications Center (SEDAC) Palisades, NY
- Wilson RT (1997) Livestock, pastures, and the environment in the Kyrgyz Republic, Central Asia. *Mt Res Dev*:57–68
- World Bank (2003) *The World Bank Annual Report 2003 (English)*. The World Bank, Washington, DC
- World Bank (2017) *The World Bank Annual Report 2017*. The World Bank
- Xi X (2014) Examination of mineral dust variability and linkages to climate and land-cover/land-use change over Asian drylands. Dissertation, Georgia Institute of Technology
- Xi X, Sokolik IN (2012) Impact of Asian dust aerosol and surface albedo on photosynthetically active radiation and surface radiative balance in dryland ecosystems. *Adv Meteorol* 2012
- Xi X, Sokolik IN (2015) Dust interannual variability and trend in Central Asia from 2000 to 2014, and their climatic linkages. *J Geophys Res Atmos*
- Xi X, Sokolik IN (2016) Quantifying the anthropogenic dust emission from agricultural land use and desiccation of the Aral Sea in Central Asia. *J Geophys Res-Atmos* 121(20):12270–12281
- Zender CS, Miller RLRL, Tegen I (2004) Quantifying mineral dust mass budgets: terminology, constraints, and current estimates. *Eos Trans AGU* 85(48):509–512
- Zhang X-Y, Gong S, Zhao T et al (2003) Sources of Asian dust and role of climate change versus desertification in Asian dust emission. *Geophys Res Lett* 30(24)